19

The Contribution of Molecular Modelling to the Knowledge of Pesticides

Ethel N. Coscarello[1], Ruth Hojvat[2],
Dora A. Barbiric[3] and Eduardo A. Castro[1]
[1]*Universidad Nacional de La Plata*
[2]*Universidad Nacional del Noroeste de Buenos Aires*
[3]*Universidad de Buenos Aires*
Argentina

1. Introduction

Evolution of computer hardware has made available massive amounts of computing power in practically all fields of chemistry. Personal computers currently have computational speed and storage capacities that exceed old supercomputers and are much cheaper. Computational Chemistry and Molecular Modelling are areas of Theoretica1 Chemistry with emphasis on application-oriented molecular problems being solved for a wide range of systems. So modelling calculations and computational chemistry have naturally entered applied sciences as for example soil science.

Most molecular modelling studies involve three stages (Leach, 2001). In the first stage a model is selected to describe the intra- and inter-molecular interactions in the system. The two most common models that are used in molecular modelling are quantum mechanics (QM) and molecular mechanics (MM). These models enable the energy of any arrangement of the atoms and molecules in the system to be calculated, and allow the modeller to determine how the energy of the system varies as the positions of the atoms and molecules change. The second stage of a molecular modelling study is the calculation itself, such as an energy minimisation, a molecular dynamics or Monte Carlo simulation, or a conformational search. Finally, the calculation must be analysed, not only to calculate properties but also to check that it has been performed properly.

The fundamental equation determining the properties of atomic and molecular systems is the Schrödinger equation. Its analytic solution is only possible for a few simple model cases, but computer programs have been developed for the quantum chemical computation of atoms and molecules. The QM approximation for the calculation of molecular properties are: ab initio and DFT (density functional theory) methods, and semiempirical methods (for an introductory level, see Atkins & de Paula, 2006). The first two ones are computationally most expensive, but they usually yield the most reliable results. Ab initio calculations use the complete and correct hamiltonian and do not use other experimental data except fundamental physical constants. The density functional method does not intend to calculate the molecular wavefunction, but calculates the electron probability density rho (ρ) and calculates the molecular electronic energy starting from rho. Semiempirical methods are computationally less expensive, they use a simpler hamiltonian in the Shrödinger equation but require parameter sets for successful application.

Force-field and interatomic potential methods are the cheapest ones. They are not quantum mechanics methods and do not use the hamiltonian operator nor a molecular wavefunction. They rely on the empirical adjustment of parameters. Molecules are usually visualized as an assembly of atoms connected by bonds, and molecular energy is expressed as a sum of terms which correspond to bond, angle, torsion, van der Waals and electrostatic interaction energies. The mathematical form of the energy terms varies from force field to force field. The potential function of the system depends on the relative positions of the atoms with respect to each other and it returns energy as a function of conformation.

Considering a single or a few molecules alone, physically corresponds to the gas phase or vacuum. Many chemical processes, however, occur in solution, on surfaces, in solid state or involve macromolecules which have many closely separated conformational energy minima and contain large numbers of atoms or molecules. Computer simulation methods enable the study and prediction of properties of such dynamic systems through the use of techniques that consider small replications of the macroscopic system with manageable numbers of atoms or molecules. The two most common simulation techniques used in molecular modelling are the molecular dynamics (MD) and the Monte Carlo (MC) methods. MD is a computer simulation technique where the time evolution of a set of interacting particles (atoms, molecules) is predicted by integrating their equations of motion, following the laws of classical mechanics (Jensen, 1999; Leach, 2001). Velocities are governed by the forces that the atoms of the system exert on each other. The force on an atom can be calculated from the change in energy between its current position and its position a small distance away. Knowledge of the atomic forces and masses can then be used to solve the equations to give the positions of each atom along a series of extremely small time steps of the order of femtoseconds (10^{-15} seconds). The resulting series of snapshots of structural changes over time is called a trajectory. Though deterministic, MD is a statistical mechanics method: it is a means of obtaining a set of configurations distributed according to some statistical distribution function, or statistical ensemble. A trajectory obtained by MD provides such a set of configurations and the value of a physical quantity is obtained as an arithmetic average of its instantaneous values assumed during the MD run.

MC method (Jensen, 1999; Leach, 2001) starts from a given geometry and a new configuration is generated by making random changes to the positions of one or more atoms. The new geometry is accepted as starting point for the next perturbing step if it is lower in energy than the current. If it is higher, it is evaluated whether it can exist in equilibrium with configurations of lower potential energy at a given temperature. This is done by calculating the ratio of populations of the two states involved (with energy separation ΔE), i.e. $\exp(-\Delta E / kT)$ where k is the Boltzmann constant. The value is compared to a random number between 0 and 1. If the factor is larger than this number, then the configuration is accepted; if the factor is not larger, the configuration is rejected and the next step is taken from the old geometry. A sequence of configurations is generated from which, for example, geometries may be selected for subsequent minimization.

MC calculations are somewhat similar to the MD calculations. But while MD simulations use an equation of motion as the basis for generating new configurations, MC simulations employ a statistical sampling technique to generate configurations that represent a trajectory. MD calculate ensemble averages by calculating averages over time, whereas MC calculations evaluate ensemble averages by sampling configurations from the statistical ensemble. In principle and in a long run, both should lead to the same average results for the same system.

This chapter is a review of selected theoretical reports that appeared during the last twelve years referred to molecular modelling applied to the field of pesticides and to some biological systems involved in their (bio)chemistry.

2. Nitrocompounds

Compounds containing one or more nitro groups are commonly used as explosives (Spain 1995), organic solvents (Scholz et al., 2005), herbicides and pesticides (Harrison et al., 2005), and drugs (Ahlner et al., 1991; Balbi, 2004). As a result, they appear as contaminants in water sources, such as surface water and industrial waste waters.

Natural adsorbents and catalysts which are based on the alumino–silica minerals and other types of soils occupy one of the most important places in the development of clean-up technologies. Clays are layer-type aluminosilicate minerals based on a two-dimensional stack of layers. These are made of either tetrahedral sheets of SiO2 motifs or octahedral sheets of metal oxide and hydroxide (where the metal can be Al, Fe, Mg) or both. Cohesion between the layers is maintained by weak electrostatic and van der Waals interactions mediated by interlayer cations and water molecules. Boulet et al. (Boulet et al., 2006) have contributed a review of the electronic structure computer simulation studies of clays, focusing on important case studies, where it was shown how ab initio calculations can help in the interpretation of experimental observation and the relationships between the structure and properties of clays. Here we offer two examples of how careful calculations and analyses of model clays interacting with nitrocompounds have been carried out.

Haderlein et al. (Haderlein, 1993; 1996; Weissmahr et al., 1997) proposed that the adsorption of nitroaromatic compounds (NACs) on clays under natural conditions was due to the NAC interaction with the siloxane sites of clays. The interaction was postulated to be electron donor-acceptor in nature: NACs (electron acceptors) interact via the electron deficient π-system with the oxygen atoms of the siloxane surface (electron donors). To further investigate this interaction, Pelmenschikov & Leszczynski (1999) performed analyses of the adsorption of 1,3,5-trinitrobenzene (TNB) with the basal siloxane surface of clay minerals by computations of molecular models at several ab initio and DFT levels of theory. Calculations were performed with the GAUSSIAN-94 package (Frisch et al., 1995), geometries were optimized and binding energies were computed. For the DFT calculations, the three parameter B3LYP functional (Becke, 1988; Lee et al., 1988) was used. The geometry of TNB and its position with respect to the surface was fully optimized within adopted symmetry constraints. The silicon-oxygen clusters mimicking the siloxane sites were constructed of SiO_4 tetrahedra with the Si-O bond length being equal to 1.61 Å, the average value for clay minerals (Bish, 1993). The border oxygen atoms of the silicon-oxygen clusters were saturated with H atoms located on the corresponding "broken" O-Si bonds, at 0.95 Å. The geometry of the surface clusters was not optimized, so the effect of the interaction on the surface geometry was neglected**.** Results suggested that the complexation of NACs with the siloxane sites of clays is mainly governed by dispersion interaction, accounted for by the planar structure of both the NACs and the siloxane surface. Due to the pair-additive character of the attractive dispersion interaction between the atoms of two interacting partners, the superimposition of plane NACs on the siloxane layer resulted in a strong stabilization effect. The averaged binding energy (38 kJ/mol) was in good agreement with the experimental data (ΔHads≈-40 kJ/mol). The energetically optimal arrangement of TNB with respect to the surface would be governed by the balance between favourable dispersion and electrostatic

forces, and repulsive exchange forces. Considering that dispersion interaction is short-range in nature, the nonplanarity of NACs with branched alkyl substituents would prevent the maximum closeness of the molecules to the surface, causing the binding to be weaker in such cases. According to the authors, the predominant role of the short-range dispersion interaction in the adsorption, justified the use of small molecular models of the siloxane surface in their study.

Leszczynski et al. (Gorb et al., 2006) introduced later a more realistic model of a clay surface, considering three ditrigonal cavities of clay montmorilonite and they calculated the components of the interaction energy of TNB with such surface. They modelled, at a quantum-chemical level, the interaction of TNB with the siloxane surface by applying the ONIOM methodology (Svensson et al., 1996). This is an n-layered integrated quantum mechanical and molecular mechanics (QM/MM) method designed to facilitate accurate ab initio calculations of large chemical species. QM/MM methods treat by different levels of theory different parts of a structure or system: usually, an important one is calculated by electronic structure methods (semiempirical, ab initio or DFT), while the less important part is calculated by a force field method. In ONIOM a typical calculation is constructed from a series of layers: e.g., an inner core may be treated with the density functional approach, the intermediate layer with a low level ab initio theory and the outer layer with a force field. So Gorb et al. represented the target cluster with the chemical formula $Al_{22}Si_{13}O_{81}H_{44}$,which was subdivided into three levels of theory, though all of them QM levels. For comparison, the interaction of TNB with a pure silicon–oxygen cluster with formula $Si_{13}O_{37}H_{22}$ was also considered, with calculations performed at the ab initio and DFT levels of theory using the GAUSSIAN 98 package (Frisch et al., 1998). The interaction energy of TNB was investigated by the authors using an energy decomposition scheme proposed by Sokalski et al. (1988): the interaction energy is partitioned into several terms, i.e. the first-order electrostatic ε'_{el} , first order exchange ε'_{ex} and high order deformation ε_{def} . The latter accounts for the charge transfer and polarization interactions. To take into account the correlation energy, an additional ε_{corr} term was also considered by the authors, aiming at the inclusion of all intermolecular and higher order correlation energy. As for the latter, ab initio calculations are based in first approximation on the one-electron model: each electron in a molecule moves in the *average* field created by the other electrons. Actually, electrons interact instantaneously and tend to avoid each other. This correlation results in a lower average interelectronic repulsion and thus a lower state energy. The difference between electronic energies calculated at lower (self consistent field, SCF) level and the exact nonrelativistic energies is the *correlation energy*. Gorb's et al. results suggest that the attractive term of the adsorption energy consists of two contributions. One is the electrostatic interaction, of specific character and responsible for the orientation of the adsorbed NAC. The other contribution, without a specific character, originates from dispersion energy. Only approximately half of the adsorption energy contributes to the specific interaction with the siloxane sites of clay minerals, which would explain the high mobility of adsorbed TNB as revealed by NMR studies (Weissmahr et al., 1997). The interaction energy decomposition was implemented in the GAMESS program (Schmidt et al., 1993). The calculations of electrostatic potential were performed and visualized by the MOLDEN program (Schaftenaar & Noordik, 2000).

Another study of inetractions with a solid surface was peformed by Wahab and Koutselos (2009), involving nitrobenzene (NB) as a model pollutant. The authors modelled the adsorption and primary oxidation step for the photodegradation of NB by using the

semiempirical MSINDO SCF MO method. This method has been documented for the first-, second-and third-row main group elements and first-row transition metal elements (Ahlswede & Jug, 1999a, b; Bredow et al., 2001). Molecular dynamics simulations of the cluster-substrate (TiO_2- $C_6H_5NO_2$) models were performed for 2000, 4000 and 6000 femtoseconds at 300 K. The adsorption geometries of NB onto TiO_2 surface were simulated focusing on the parallel and perpendicular conformations. The computed energies of both adsorption modes indicated that the adsorption process is exothermic. The authors found that the adsorption energy is influenced by the substrate geometry and that the perpendicular conformation is favoured through a preferential interaction between the oxygen atoms of NO_2 group and the surface of TiO_2. The quantum chemical calculations of the heterogeneous oxidation of NB required an extended saturated cluster for the modelling of the anatase TiO_2 (100) surface such as $Ti_{36}O_{90}H_{36}$. The authors also analysed the primary steps of the oxidation of NB by OH radical, in the homogeneous gas phase (photochemical) and on the anatase TiO_2 surface (photocatalytic). In order to identify the primary OH initiated photooxidation intermediates, they employed two different theoretical approaches which revealed that the *meta*-hydroxynitrocyclohexadienyl radical is energetically more favoured than the analogous *para*- and *ortho*- radicals for the photochemical photolysis, following the expected selectivity rules. As for photocatalysis, the OH radical attack appeared to be non-selective and all three possible isomers showed comparable stabilities.

Although nitro compounds are of general and biological significance, only a limited number of studies have focused on developing force field (FF) parameters for use in molecular simulations (Michael & Benjamin, 1998; Janssen et al., 1999; Price et al., 2001; 2005; Jorge et al., 2006). Price et al. (2001) developed nitro-parameters for the OPLS-AA FF (Jorgensen et al, 1988; 1996) that resulted in good agreement with experimental gas-phase and liquid properties, e.g., density, heats of vaporization, and free energies of salvation, from molecular simulations. A comparison of nitrobenzene FFs and experiment was discussed by Jorge et al. (2006), who found that OPLS-AA compares most favourably with observations.

For the CHARMM FF (Brooks et al., 1983), Klauda & Brooks (2008) developed nitro-parameters consistent with CHARMM optimization procedures (MacKerell, 2001; 2004; 2005). Their new parameter set, referred to as C27rn, was then tested on pure liquid and interfacial systems of nitroalkanes and nitrobenzene. Special focus in the FF development was on potential energy scans of two nitro torsional angles, i.e., C-C-N-O and C-C-C-N. Therefore, highly accurate ab initio methods were used to describe the conformational energies of nitroalkanes and nitrobenzene. The Gaussian03/Rev. B.03 suite of programs (Frisch et al., 2004) was used for the QM calculations and the FF was adjusted accordingly to best match them. MD simulations were performed with CHARMM using C27r for the alkane portion of the FF (Klauda et al., 2005a, b) and adjustments to the nitro FF, i.e. C27rn. Simulations yielded an increased population (74%) of *gauche* conformers compared to OPLS-AA, as the calculated *gauche* conformer of the C-C-C-N torsion resulted more stable than the *trans* one. Bulk and interfacial properties from the nitro simulations with C27rn, such as densities, heats of vaporization, and surface tensions, were in agreement with experiment. However, the calculated diffusion constant of liquid nitrobenzene with both OPLS-AA and C27rn was lower than in experiment. Since these new parameters accurately represent interaction energies between water and nitro compounds and pure component properties, C27rn was proposed to be used in simulations of biologically relevant compounds.

3. Organophosphorous compounds

There is an increasing interest in developing strategies for the detection and detoxification of organophosphorous compounds (phosphorus-containing organic chemicals). They are often used as pesticides and warfare agents. Because of their high toxicity, there is a serious demand for more-sophisticated and useful techniques for the detection and decomposition of these substances, as well as for information about their (thermo)chemical properties or behaviour.

In order to evaluate the ability of beta-cyclodextrin (β-CD) to discriminate between different enantiomers of pesticides, Manunza et al. (1998) carried out molecular dynamics (MD) experiments to investigate the mechanism of selective binding of β-CD with the R or S enantiomers of dichlorprop, 2- phenoxypropionic acid and dioxabenzofos. The dichlorprop and the 2-phenoxypropionic acid molecules are similar as both have a phenyl ring with a substituent bearing a carboxylic function. Molecular structures were constructed and six inclusion 1:1 complexes were formed, one for each enantiomer, after a docking process into the cavity was performed. These adducts were the starting structures in the MD experiments. The MD runs were performed employing the DLPOLY2 (Smith & Forester, 1994) program. The AMBER (Weiner et al., 1984; Cornell et al, 1995) plus GLYCAM (Woods et al., 1995) force field was used with the necessary adaptations, while the β-CD partial atomic charges were calculated by the Gasteiger method (Berendsen et al., 1981). The starting β-CD structure for the simulation was taken from the "BCDEX04" entry of the Cambridge Crystallographic Database. All the MD simulations were performed in the NVT ensemble (constant number of particles, volume and temperature) inside a 35 Å cubic cell at a temperature of 298 K. The system was allowed to equilibrate for 200ps and the trajectory was collected over 1000ps. Results account for the formation of adducts with the dichlorprop and the 2-phenoxypropionic acid molecules which are stable at room temperature, while neither of the dioxabenzofos enantiomers entered the β-CD cavity completely. Computational results agreed with the experimental evidence that β-CD forms stable complexes with both dichlorprop and 2-phenoxypropionic acid after 7 h at 70^{o}C and after 24h at room temperature, whereas no experimental evidence was observed for dioxabenzofos complexation. The energetic data indicated that the β-CD molecule shows preference for S enantiomers. The plots of the radial distribution functions showed that the R enantiomers form hydrogen bonds mainly with the oxygen atoms of the secondary hydroxyl groups in the β-CD, while the S enantiomers formed H-bonds even with the oxygens in the primary hydroxyl groups of the cycle. Energy data revealed that complexes with the R enantiomers of dichlorprop and 2- phenoxypropionic acid exhibit a more advantageous H-bond network, and that adducts with the S enantiomers form by the release of strain energy mainly by the β-CD molecule.

The application of cyclodextrins to pesticide formulation was, until recent years, rather modest (Szejtli, 2004), but the situation has significantly changed since the cost of technical quality β-CD, entirely acceptable for the pesticide formulation industry, has declined. So potential use of β-CD could be of great interest to enhance biological activity of these chemicals (Nair et al., 2006). The alkaline hydrolysis of three organophosphorous pesticides, i.e. fenitrothion, parathion and methylparathion, appears to be inhibited by β-CD (Vico et al., 2002). This effect, ascribed to a shallower inclusion of the guest in the cavity, is lower in the case of fenitrothion (Kamiya et al., 1995). Induced circular dichroism analysis revealed that the inclusion of the pesticides occurs by the nitro group and the same happens with the

analogous carboxylic esters, whose hydrolysis is, contrarily, catalyzed by β-CD (Osa & Suzuki, 1996). Coscarello et al. (2009) analyzed the complexation process of both pesticides and their carboxylic ester analogues by β-CD. The authors applied molecular mechanics and the PM3 (Stewart, 1989a; b) semiempirical methods contained in the Hyperchem-7 (2002) program. The complexation of fenitrothion was further explored, since experiments proved that its hydrolysis is relatively less inhibited and progresses mainly through a different pathway. Results showed that complex structures involving the carboxylic esters enable effective interactions between the guest carbonyl and the rim of the host. Methylparathion and parathion, however, appeared deeply included in the cavity of β-CD, so conditions for a nucleophilic attack by the β-CD would not be favourable. As for fenitrothion, different complex geometries were yielded, none being apparently prone to an attack by the β-CD, but favouring instead the approach of an external OH^- group, according with experiment.

Dichlorvos (2,2-dichlorovinyl phosphate, DDVP) is a widely used organophosphorus insecticide. DDVP may be released into the atmosphere and can also be released into the environment as a major degradation product of other organophosphate pesticides, such as trichlorfon (Murphy et al., 1996)) and metrifonate (Hofer, 1981; Pettigrew et al., 1998). The reaction of DDVP with atmospheric OH radicals is considered to be a dominant removal process for gaseous DDVP. Knowledge of the OH-initiated DDVP oxidation mechanism and the major degradation products is limited. Feigenbrugel et al. (2006) detected phosgene (Cl_2CO) and carbon monoxide (CO) and proposed a possible reaction mechanism to explain the observed products, in which CO formation is initiated by H abstraction from the CH_3O group of DDVP, and then the product radical may further react with O_2/NO leading to HCO. The observed CO would be formed through the reaction of HCO with O_2. The formation of Cl_2CO would be initiated via OH addition to the carbon-carbon double bond. Zhang et. al (2007) carried out a theoretical study on the OH-initiated atmospheric photooxidation reaction of DDVP. High-level ab initio molecular orbital calculations were carried out for the OH-initiated atmospheric photooxidation of DDVP in the presence of O_2 and NO, and using the Gaussian 03 package (Frisch et al., 2004). The geometrical parameters of reactants, transition states, intermediates, and products were optimized at the TPSSh density functional level (Staroverov et al., 2003; Tao et al., 2003). The vibrational frequencies were also calculated to determine the nature of the stationary points, the zero-point energy (ZPE), and the thermal contributions to the free energy of activation. Each transition state was verified to connect the designated reactants with products by an intrinsic reaction coordinate (IRC) analysis (Fukui, 1981). The energies of various species were determined more accurately, for a more accurate evaluation of the energetic parameters. The profile of the potential energy surface was constructed and possible secondary reaction pathways were also studied to find the mechanism of formation of secondary pollutants from the OH-initiated atmospheric reaction of DDVP. Because of the absence of experimental information on the thermochemical parameters for the reaction system, the authors calculated the standard formation enthalpies, $\Delta_f H^0(298)$, of CCl_2O and PCl_3 . The calculated values were in agreement with the available experimental ones (Curtiss et al., 1997; David, 2007). On the basis of the product yields of CCl_2O and CO, Feigenbrugel et al. had suggested that H abstraction from the CH_3O group accounts for 43% of the overall reaction and that OH addition to the >C=C< bond accounts for 47% of the overall reaction. Zhang et al., however, found that four product pathways are energetically feasible for the degradation of DDVP initiated by atmospheric OH radicals. In addition to CCl_2O and CO, HO_2 and a closed-shell organophosphorous compound denoted P10 would be also easily produced from the

pathway initiated by H abstraction from the CH_3O group, and CCl_2CHO and $(CH_3O)_2P(O)OH$ are also energetically feasible products from the pathway of OH addition to the >C=C< bond. Thus, the authors inferred that calculation of the branching ratios of H abstraction from the CH_3O group and OH addition to the >C=C< bond only from the productivities of CCl_2O and CO, would not be reasonable.

Inorganic metal oxides are well-known for their use in chemical industry as adsorbents, sensors, catalyst, etc. Because of their unique morphological features and high surface area, nanocrystals of metal oxides were used as adsorbents for decomposition or detection of variety of pollutants and harmful substances, including organophosphorous compounds (Richards et al., 2000). Recently, zinc oxide (ZnO) nanoparticles have received much attention, because of applications such as ultraviolet absorption, decomposition, deodorization, and antibacterial treatment. It is a well-known catalyst, adsorbent, toxic gas sensor, etc. (Yun et al., 2005). Among the unique chemical properties of ZnO is that it lies on the borderline between ionic and covalent solids (Duke et al., 1977). Leszczynski et al. (Paukku et al., 2009) studied the adsorption of Tabun (TB) -a nerve agent- and of dimethyl methylphosphonate (DMMP) -an organophosphorous simulant- on polar and nonpolar ZnO surfaces, using the cluster model approach. Different cluster sizes and adsorption sites of ZnO were considered, and the influence of different computational methods on the nature of interactions of these molecules with the crystal surface of ZnO was investigated. Two types of surfaces, polar and nonpolar, were considered for ZnO, the latter being the most stable one for the solid. These ZnO surfaces have been studied experimentally (Duke et al., 1977; 1978). Calculations of adsorption of DMMP and TB on the model surfaces of ZnO were conducted at several ab initio levels of theory, and using the ONIOM method as implemented in the Gaussian 03/Rev.C02 program package (Frisch et al., 2004), in order to test the influence of the method on the intermolecular interactions. The geometries of the target molecules were fully optimized while the ZnO fragment was kept frozen. DMMP contains three different groups that can be involved in the intermolecular interactions with the active sites of the ZnO surface: P=O, O-CH3, and CH3. Therefore, several different initial orientations of DMMP toward the oxide cluster were tested. To test the effect of the surrounding Zn and O atoms and additional layers on the adsorption of the target molecule, the authors performed the ONIOM calculations: the molecular system was divided into two layers, which were treated at different levels of theory, DFT and PM3 methods. From the results, the authors concluded that on both ZnO surfaces, the molecular adsorption proceeds as chemisorption via the formation of a Zn····O chemical bond in the case of the DMMP adsorption complex, and a P····O covalent bond or a Zn····N chemical bond for TB adsorption complexes. The type of surface greatly affected the strength of the intermolecular interactions and the interaction energies. The results indicated that the adsorption of DMMP and TB is energetically more favourable on the nonpolar ZnO surface. TB was determined to be bound more tightly to the ZnO surface than DMMP, but the adsorption energies were approximately twice as low as the values revealed for the adsorption of TB and DMMP on the CaO surface, as reported previously by the same authors (Michalkova et al., 2007; Paukku et al. 2008). Therefore, conclusion was that the decomposition of these compounds would proceed easier on CaO, whereas ZnO should be an efficient sensor for their detection.

The experimental enthalpies of formation ($\Delta_f H°(298)$) for many important organophosphorous compounds are often unknown or known with relatively large uncertainties, due to incomplete combustion and formation of a mixture of the various phosphorous oxyacids that make difficult the precise definition of the final system (Pilcher,

1990). Because of the lack of accurate thermochemical data, alternative approaches, such as quantum chemical calculations should be used to predict the $\Delta_f H°(298)$ values for organophosphorous compounds. To predict accurately thermochemical properties for larger molecules at relatively low computational cost, the composite Gaussian-*n* [G2, G3, G3(MP2), G3X, G3X(MP2), etc.] methods were developed (Curtiss et al., 1998, 2000a, 2000b, 2001) (Baboul et al., 1999). In these methods, calculations from different levels of theory are combined in order to produce energy differences accurate to about 1 kcal/mol, as compared to experimental results. They have been calibrated on a reference set of atomic and molecular properties (atomization energies, ionization potentials, electron and proton affinities, etc.). The general principle is to perform a calculation at a high level of theory and then correct this value for deficiencies using less expensive, lower level theories.

The modification of the G3 theory, in particular, called Gaussian-3X (G3X), was designed to improve the agreement between theoretical and experimental $\Delta_f H°(298)$ for molecules, which contain second row atoms (Na-Ar). This method gives a good agreement with experiment for inorganic phosphorus compounds. Dorofeeva & Moiseeva (2006) calculated the $\Delta_f H°(298)$ of organic compounds containing phosphorus. Their purpose was: a) to assess generally accepted experimental data on organophosphorus(III) compounds using the G3X method; b) to recommend a set of consistent $\Delta_f H°(298)$ values based on best quality experimental values and G3X results; c) to calculate accurate $\Delta_f H°(298)$ values for organophosphorus(III) compounds with missing experimental thermochemical data; d) to derive a consistent and accurate set of group activitiy values (GAVs) needed to estimate the $\Delta_f H°(298)$ of larger organophosphorus(III) molecules, account taken that the empirical group additivity method of Benson (Benson et al., 1969) (Cohen & Benson, 1993) can predict the thermochemical properties of organic compounds with chemical accuracy, i.e. within 4 kJ/mol. So the $\Delta_f H°(298)$ of 55 organophosphorus(III) compounds were calculated at the G3X, G3X(MP2), and DFT levels of theory using the atomization energy procedure and the method of isodesmic reactions. This method is based on the principle that, for a given reaction, a particular computational approach can be expected to have similar deficiencies for both reactants and products that are chemically similar; thus, deficiencies are expected to cancel appreciably when the enthalpy of a reaction is calculated. Dorofeeva & Moiseeva calculated as well, the $\Delta_f H°(298)$ values for 50 moderate sized molecules with 2-10 non-hydrogen atoms directly from the G3X atomization energies. Examples of such group are $P(CH_3)_3$, $P(C_2H_5)_3$, $P(OCH_3)_3$, $n\text{-}C_4H_9OPCl_2$, $[(CH_3)_2N]_2PCl$, $(C_2H_5)_2\text{-}NPCl_2$, and $[(CH_3)_2N]_2PCN$. By comparison of the available experimental data with the G3X results, it was found that the G3X method succeeded in reproducing well established $\Delta_f H°(298)$ to an accuracy of ±10 kJ/ mol. A good agreement between the known experimental values and G3X results for 14 compounds provided support to the predictions for remaining species with unknown experimental $\Delta_f H°(298)$ or known with large uncertainties. The $\Delta_f H°(298)$ values obtained in this work provided a consistent set of reliable estimates for the thermodynamic modelling of processes involving phosphorus(III) containing species. The recommended $\Delta_f H°(298)$ values were used to derive the GAVs for 45 groups involving the phosphorus(III) atom and thus extending the applicability of Benson's group additivity method to estimate the $\Delta_f H°(298)$ of larger organophosphorus(III) compounds (for which high level quantum chemical calculations could appear impracticable).

Hemelsoet et al. (2010) performed a comprehensive ab initio study on phosphorus-containing species with three primary aims: a) to assess a broad variety of current computational methods to determine an appropriate level of theory for the calculation of

reliable bond dissociation properties of phosphorous compounds; b) to provide thermochemical data such as the enthalpy of formation, the heat capacity and the entropy for a set of phosphorus-containing species representing industrially important coke-inhibiting additives; c) to compute bond dissociation enthalpies (BDEs) of these compounds to establish the stability of the formed radicals and their reactivity trends. Standard ab initio molecular orbital theory and density functional theory calculations were carried out using the Gaussian03/Rev. D.01 (Frisch et al., 2004), Molpro 2002.6 (Werner et al., 2002), and NWChem5 (Bylaska et al., 2007) software packages. Geometries were optimized at the DFT level of theory. Harmonic vibrational frequencies were computed at the same level of theory and were used to provide zero-point vibrational energies and to confirm the nature of the stationary points. Subsequent single-point energy calculations were performed using a variety of levels of theories and several methods were tested for their performance. It was shown that the composite G3(MP2)-RAD (Hodgson & Coote, 2005) method generates heats of formation of small phosphorus-containing molecules that are in good agreement with experimental data. Hodgson & Coote investigated the relative stabilities of phosphoranyl radicals •P(CH3)3X and introduced a new measure of stability, i.e., the α-radical stabilization energy (α-RSE). As opposed to the standard RSE definition, the α-RSE measures the stability of the radical with respect to P(CH3)2X instead to H-P(CH3)X. This means that it assesses the stability of the radical on the basis of its susceptibility to α-scission of the methyl radical rather than to hydrogen abstraction. The study provided a large set of high-level calculated data that were taken as benchmark values by Hemelsoet et al.. The bond dissociation energies D(•P-C) and D(•P-X) of the phosphoranyl radicals •P(CH3)3X were calculated. The benchmark values of the D(•P-C) group could accurately be reproduced using various low-cost DFT methods, whereas this was much more difficult for the D(•P-X) values. In the case of D(•P-C), the ROB2PLYP (Grimme, 2006) and ROMPW2PLYP (Schwabe & Grimme, 2006) methods performed the best. The D(•P-X) values, on the other hand, were overall best reproduced using the SOS- (Jung, 2004) and SCS-ROMP2 (Grimme, 2003) methods. The RO prefix designs calculations on radicals that were performed with a restricted-open-shell reference wave function, as opposed to the unrestricted-open-shell computations. Bond dissociation enthalpies were calculated using the BMK (Boese & Martin, 2004), M05-2X (Coote & Henry, 2005) , and SCS-ROMP2 level of theory. The three methods give the same stability trend. No correlations between BDEs and geometrical parameters or atomic (spin) charges were obtained. The BDEs of the phosphorus(III) molecules were found to be lower than their phosphorus(V) counterparts. Overall, the authors report the following found ordering: BDE(P-OPh) < BDE(P-CH3) < BDE(P-Ph) < BDE(P-OCH3). Additionally, standard enthalpies of formation, entropies and heat capacities of a set of ten organophosphorous species, representing coke-inhibiting additives, were computed using the low-cost BMK functional. Results were consistent with available experimental data and could be used as input in single-event kinetic models.

4. Enzymatic activity

Among the chemical classes that have been developed as pesticides, organophosphorous compounds (together with carbamates), represent the most significant share of the world pesticide market (Casida & Quistad, 1998). Both classes owe their acute toxicity to the inhibition of acetylcholinesterase (AChE), enzyme that regulates the concentration of the neurotransmitter acetylcholine (ACh). The principal role of AChE is in the nervous system,

where it serves to terminate impulse transmission at cholinergic synapses by hydrolysis of the neurotransmitter acetylcholine at nearly diffusion-limited rates (Silman & Sussman, 2005). The enzyme phosphotriesterase (PTE) has the ability to hydrolyze a wide range of organophosphate triester compounds including pesticides and insecticides as well as chemical warfare agents, and it has a great potential for use in bioremediation of environmental contaminants.

Koča et al. (2001) examined theoretically the geometry and mobility of various PTE active site-substrate complexes, with paraoxon and sarin, as the chosen substrates. Observations indicated that the positioning of the substrate in the active site of the enzyme, as well as the flexibility of the active site, play important roles in the enzymatic process. As the enzymatic reaction is very fast, obtaining direct experimental data about the enzyme/substrate complex is difficult , so the authors recurred to molecular dynamics (MD) simulations on solvated PTE-substrate complexes, as well as quantum mechanical calculations on a simplified model of the active site complexed with the substrates, to address questions about the protein behaviour before and when interacting with the substrate. MD simulations were carried out on subunit of the PTE dimer, using AMBER 5.0 (Case et al., 1997) with the force field reported by Cornell et al (1995). In the current work, seven 500-picoseconds simulations were produced, five on the fully solvated protein and two on the gas-phase substrates, paraoxon and sarin. Partial atomic charges for paraoxon, sarin, and the carbamylated Lys-169 of the active site were determined by using the restrained electrostatic potential (RESP) procedure (Cornell et al., 1995). Quantum chemical calculations were carried out by using the Gaussian94 (Frisch et al., 1995) and Gaussian98 (Frisch et al., 1998) programs. Geometries of the PTE-substrate complex models were fully optimized by employing DFT theory, B3LYP functional (Becke, 1988; Lee et al., 1988). The corresponding vibrational frequencies were evaluated at the optimized geometries to verify their true stability. The results obtained from the molecular dynamics simulations showed that multiple orientations of paraoxon and sarin in the active site of zinc-substituted PTE are possible. The phosphoryl oxygen becomes strongly coordinated to the less buried zinc cation –there are two present in the active site-, which allows for strong polarization of the reaction center of the substrate. These results indicate that the enzymatic hydrolysis occurs as a multistep process, in which formation of the substrate-protein complex is the first step. There are conformational changes that occur throughout the active site region of PTE when the enzyme is immersed in the water bath and relaxed by MD. The most remarkable change is the opening of the gateway in a pocket where the location of the leaving group is expected. The enzyme's gateway opens with and without substrate being present in the active site. The size of the opening is dependent on the substrate and may range from 11 to 18 Å. Different conformational behaviors are observed for the same substrate substituents within different pockets, for different simulations, as well as in the gas phase. This shows that the active site pockets generally contribute to the substrate binding. Detailed analysis of all trajectories revealed that this contribution in not based on hydrogen bonding. The pockets, in which the substrate substituents are localized, thus exhibit different flexibility and interact with the substrate with coordinated conformational adjustments.

Wong & Gao (2007) also undertook the PTE hydrolysis of paraoxon to determine the potential of mean force (PMF), by using a dual-level QM/MM approach. The intrinsic (gas-phase) energies of the active site in the QM region were determined by using density functional theory (B3LYP) and second-order Møller-Plesset perturbation theory (MP2)

(Hehre et al.,1986); the molecular dynamics free energy simulations were performed by using semiempirical QM/MM interactions, i.e. the mixed AM1:CHARMM potential (Dewar et al., 1985; 1988; 1989) (MacKerell, 2001; 2004; 2005). As already mentioned, a key feature of the active site of PTE is the binuclear zinc center, in which each zinc ion is coordinated to five ligands in a distorted trigonal bipyramidal structure. The simulation results suggested that the reaction free energy profile is mirrored by structural motions of the binuclear metal center in the active site. A carbamylate group from Lys169 and the nucleophile hydroxide ion both form bridged coordinations to the two zinc ions in a compact conformation with an average zinc-zinc distance of 3.5 ± 0.1 Å. The P─O bond of the substrate paraoxon is activated by adopting a tight coordination to the more exposed Zn_{β}^{2+} ion, and releases the coordinate to the hydroxide ion, increasing its nucleophilicity. The result is a loose binuclear conformation, characterized by an average zinc-zinc distance of 5.3± 0.3 Å at the transition state and the product state. It was also found that a water molecule enters into the binding pocket of the loosely bound binuclear center, originally occupied by the nucleophilic hydroxide ion. It was suggested that the proton of this water molecule is taken up by residue His254 of the PTE at low pH or released to the solvent at high pH, resulting in a hydroxide ion that pulls the Zn_{β}^{2+} ion closer to form the compact configuration and restores the resting state of the enzyme.

Taking into account that the non-harmful transformation of hazardous chemicals, such as organophosphorous compounds, could also be attained by enzymatic biodegradation (Raushel, 2002), Leszczynski et al. (Dyguda-Kazimierowicz et al., 2008) focused on the comprehensive ab initio study of possible gas phase mechanisms of the alkaline hydrolysis of bacterial PTE substrates, regarding bonds such as:

a. P─O, phosphorus-oxygen (e.g., *O*,*O*-diethyl *p*-nitrophenyl phosphate (paraoxon), *O*,*O*-diethyl *p*-nitrophenyl thiophosphate (parathion)),
b. P─F, phosphorus-fluorine (e.g., *O*,*O*-diisopropyl phosphorofluoridate (DFP), *O*-isopropyl methyl phosphonofluoridate **(**sarin, SA)),
c. P─S, phosphorus-sulfur (e.g., *O*,*S*-dimethyl *N*-acetyl phosphoramidothioate (acephate), *O*,*O*-diethyl *S*-2-ethylthioethyl phosphorothioate (demeton-S)), and
d. P─CN, phosphorus-cyanide (e.g., *O*-ethyl *N*,*N*-dimethyl phosphoramidocyanidate (tabun, TB))

Given the chemical diversity of PTE substrates, the authors deemed it essential to elucidate common features, if any, in the hydrolysis process that allow all of these substrates to be accommodated in the PTE active site and subsequently be subjected to catalysis. Hydrolysis of a P─O bond can be interpreted as an S_N2-like concerted associative mechanism, which along with the apparent involvement of a hydroxide as a nucleophile, was used to rationalize the authors' approach to utilize gas phase results for alkaline hydrolysis as a reasonable starting point for the study of the reaction occurring in the PTE active site. As for the analysis of P─F bond breakdown, though DFP and SA were selected, *O*,*O*-dimethyl phoshorofluoridate was chosen as a model compound for a preliminary study of reaction pathways. The model of demeton-S was also simplified by truncation of the last methyl group belonging to the S-2-ethylthioethyl moiety. Finally, the influence of solvent on the relative stability of structures occurring along particular reaction coordinates was examined.

The gas phase reaction profiles were studied at the ab initio level. For all the first-order saddle points, intrinsic reaction coordinate (IRC) calculations were performed, revealing the geometries of the local minima associated with a given transition state. Thermodynamic

properties (enthalpies and Gibbs free energies) were determined from vibrational frequencies computed at the fully optimized structures of stationary points along a reaction coordinate. To account for the influence of aqueous solvation, the polarizable continuum model (PCM) was applied (Mennucci et al., 2002). All calculations were performed using the Gaussian 03/Rev. C02 program. (Frisch et al., 2004). Conclusions were: 1) While all base-catalyzed hydrolysis reactions that were studied appear to follow an associative mechanism, the cleavage of P─O and P─S bonds (except of acephate molecule) occurs according to a one-step direct-displacement mechanism involving the presence of a single S_N2-like transition state. The hydrolysis of P─F and P─CN bonds, however, is consistent with an addition-elimination scheme employing several trigonal bipyramidal intermediates. 2) Except for acephate, two alternative reaction pathways are possible for each of these mechanisms that differ in the position of the attacking hydroxide relative to the phosphoryl oxygen atom. Apparently, the most energetically favourable reaction coordinate involves the hydroxide proton being stabilized by a phosphoryl oxygen. Which mechanism will occur inside the PTE active site remains, according to the authors, undisclosed. 3) In the case of a multistep addition-elimination mechanism, relatively significant energy barriers are associated with the nucleophilic attack of a hydroxide (i.e., formation of the first intermediate) and the departure of a leaving group (i.e., decomposition of the final intermediate). Judging from the results of *O*,*O*-dimethyl phoshorofluoridate hydrolysis, the energy barriers for conformational transitions are of minor importance relative to the chemical steps encompassing the formation or breakage of a chemical bond. 4) The rate-limiting step of multistep mechanisms appears to be associated with an intermediate formation. 5) Since all the reaction pathways considered constitute variants of an associative mechanism of hydrolysis, they could presumably be accommodated by a common active site of PTE.

Sensory technology has enabled the development of recyclable enzyme-based biosensors, through the confinement of enzimes within nanomaterials (Lei et al., 2002; Cao, 2005). The bacterial enzyme organophosphorous hydrolase (OPH), another name of PTE, is a candidate to be immobilized because it detoxifies organophosphorous compounds catalytically. In OPH active site -with two divalent metal ions bridged by a water molecule and a carbamylated Lys169 residue- Zn^{2+} is the native metal, but activity is also achieved via substitution by Co^{2+} , Cd^{2+} , Mn^{2+}, or Ni^{2+} (Ombrugo et al., 1992; Rochu et al., 2004). OPH catalyzes the cleavage of P─O, P─F, and P─S bonds in a variety of organophosphate triesters and related phosphonates. The immobilization of OPH in functionalized mesoporous silica (FMS) was shown to enhance stability and increase enzyme catalytic activity by 200% as compared to OPH free in solution (Lei et al., 2002), but the effect of confinement on the catalytic activity of enzymes is not clearly understood. Gomes et al. (2008) developed models of confinement and carried out MD simulations for OPH free in solution (OPH_{free}), OPH confined through atom positional constraints (OPH_{fix}) and through the coarse-grain representation of the FMS pore (OPH_{fms}). The molecular model of the enzyme OPH was built from crystallographic coordinates. Atoms were represented by a van der Waals atomic model containing atom-centered point charges. The AMBER force field (Cornell et al., 1995) was used to treat bonded and non-bonded interactions. Zinc ions in the active site were treated using a non-bonded model, while partial atomic charges and parameters for the carbamylated Lys169 were calculated as described by Soares et al. (2007).

The interactions between OPH and the FMS have steric and electrostatic components. Steric interactions, due to the inert nature of the silica material, were approximated by a non-atomic model where the positions of N-atoms of lysine residues were harmonically constrained (except Lys169). Lysine side-chains are the linkage sites in covalently linked OPH-FMS complexes (Lei et al., 2007). Electrostatic interactions, due to functionalization of the mesopore, were modelled as a cylindrical, uniform array of atoms, each atom corresponding to a given functional group. As for the $COO^{-}(CH_2)_n$ group, experimentally used to functionalize the mesoporous silica, the pore surface was represented by -1 charged point particles and van der Waals parameters corresponding to a carboxylate anion derived from the AMBER force field. The OPH structure was docked to the FMS pore wall based on the complementarity of their electrostatic potential surfaces calculated with the program APBS (Baker et al., 2001). Within simulation times of 5 nanoseconds, several structural properties reached convergence. All simulations were performed with the NWChem program (Bylaska et al., 2006) and the analyses of molecular trajectories were carried out with the GROMACS program (Lindahl et al., 2001). The OPH_{fix} simulation seemed to better describe the pool of configurations around the X-ray structure. However, this positional constraint model suppressed the flexibility of the loop region located in the entrance of the enzyme active site with the carbamylated Lys169 that coordinates the Zn^{2+} cations required by OPH for full catalytic activity; and it also suppressed the conformational fluctuations of the whole enzyme in a non-selective fashion, which would translate into a decrease of catalytic efficiency (Boehr et al., 2006). The interaction between the coarse-grained FMS model and the all-atom OPH enzyme appeared not to affect any native state motions of the free enzyme. A coarse-grain representation of the functional groups would yield a more homogenous description of the charge distribution along the silica mesoporous material, but the resulting average potential of mean force should be equivalent to that of an atomistic model. According to the authors, a physical representation of the mesoporous material, instead of the positional restraint approach, will be crucial to determine diffusion coefficients or collision rates in the confined environment. So the multiscale approach appears as a viable model for more tangible simulations of confined proteins. Such an approach allows complex biological phenomena to be modelled at different scales, attaining simultaneously accuracy and economy. These range from the sub-atomic scales of quantum mechanics, to the atomistic level of molecular mechanics, molecular dynamics and Monte Carlo methods, and even mesoscale modelling.

Recently Kwasnieski et al. (2009) analysed directly the interaction of tabun with AchE. As mentioned above, AChE catalyzes hydrolysis of acetylcholine in choline and acetic acid and thus regenerates cholinergic neuron. The catalytic site is inside a gorge of about 20 Å; the catalytic cycle involves a catalytic triad composed of three residues Ser203, His447, and Glu334 in mouse AChE. The oxyanion hole composed of Ala204, Glu121, and Glu122 is very important as it activates the substrate via hydrogen bonds (Warshel et al. 1989; Fuxreiter & Warshel, 1998). Disfunctions of AChE due to organophosphorous compounds are a major threat because they inhibit AChE irreversibly leading to convulsions, and possibly death by asphyxiation. A covalent bond is formed between the oxygen of Ser203 and the phosphorus of the organophosphorous compound. It is commonly accepted that the leaving group is *anti* to the oxygen of Ser203. Tabun reactivity is particularly interesting as tabun-inhibited AChE is one of the more difficult complexes to reactivate. Also, tabun is produced as a

mixture of two enantiomers, and one of them is 6.3 times more potent. In order to understand whether the kinetics differ for the two enantiomers or it is a different binding mechanism, the authors studied theoretically tabun inhibition of AchE by examining four possibilities for tabun fixation modes: either the fixation of the (*S*) tabun enantiomer with the cyano group *anti* or *syn* to the oxygen atom of Ser203 (S-Syn and S-Anti); or the (*R*) tabun enantiomer with the cyano group *anti* or *syn* to the oxygen atom of Ser203 (R-Syn and R-Anti). The authors used a hybrid quantum mechanics/molecular mechanics (QM/MM) methodology. Calculations were performed using BP86 (Becke, 1988) functional. Single points were also done with B3LYP and PBE0 (Adamo, 1999) functionals. Four possible attacks of tabun on the oxygen of Ser203 were studied using two crystallographic structures (PDB codes 2C0P and 3DL7): (*S*) tabun with the cyano group *syn* to the oxygen of Ser203 and (*R*) tabun with the cyano group *anti*, corresponding to the experimental X-ray structure; (*S*) tabun with the cyano group *anti* to the oxygen of Ser203 and (*R*) tabun with the cyano group *syn*, leading to a different isomer than was experimentally seen. The two X-ray structures (PDB 2C0P and 3DL7) gave analogous results for the calculations previously described. Using the PDB 2C0P, the fixation of the two enantiomers lead to the experimental X-ray structure, namely, S-Syn and R-Anti with a mechanism going through an addition elimination pathway. The kinetically determinant step appeared to be the cyano group departure, as tabun fixation on Ser203 departure is almost barrierless. As for the PDB 3DL7 structure, four possible attacks of tabun on the oxygen of Ser203 were considered: S-Syn and R-Anti, which led to the experimental X-ray structure, and S-Anti and R-Syn, which led to the isomer which has opposite relative positions of the *N*-dimethyl group and the ethoxy group in the active site as compared to the experimental structure. It appeared that the most active enantiomer is S-Syn. Thus it seems that the cyano group does not leave *anti* to the oxygen of Ser203, as expected, due to repulsive polar interaction between cyanide and aromatic residues in the active site, in particular residues Phe295, Phe297, and Phe338.

From the preceding reports, two aspects are noticeable about theoretical studies of enzymatic mechanisms involved in pesticide metabolism and degradation: they contribute both to foresee and to modulate the toxicity of waste; and they promote the use of different strategies regarding the use of enzymes in the decontamination of the environment.

5. References

Adamo, C. & Barone, V. (1999). Toward reliable density functional methods without adjustable parameters: The PBE0 model. *J. Chem. Phys.*, 110, 6158-6170.

Ahlner, J.; Andersson, R. G. G.; Torfgard, K.; Axelsson, K. L. (1991). Organic Nitrate Esters-Clinical Use And Mechanisms Of Actions. *Pharmacol. Rev.*, 43, 351-423.

Ahlswede, B.; Jug, K. (1999a). Consistent modifications of SINDO1: I. Approximations and parameters. *J. Comput. Chem.*, 20, 563–571.

Ahlswede, B.; Jug, K. (1999b). Consistent modifications of SINDO1: II. Applications to first- and second-row elements. *J. Comput. Chem.* 20, 572–578.

Atkins, P. & Paula, J.d. (2006). *Physical Chemistry*, 8th Ed., Oxford University Press, ISBN 9780198700722 ISBN 0198700725, United States.

Baboul, A. G.; Curtiss, L. A.; Redfern, P. C.; Raghavachari, K. (1999). Gaussian-3 theory using density functional geometries and zero-point energies. *J. Chem. Phys*., 110 (16), 7650-7657.

Baker, N.A.; Sept, D.; Joseph, S.; Holst, M. J.; McCammon, J. A. (2001). Electrostatics of nanosystems: application to microtubules and the ribosome. *Proceedings of the National Academy of Sciences,* 98 (18), 10037–10041, August 2001, USA.

Balbi, H. J. (2004). Chloramphenicol: A review. *Pediatr. Rev*., 25, 284-288.

Becke, A.D.(1988), Density-functional exchange-energy approximation with correct asymptotic behavior, *Phys. Rev. A*, 38 (6), 3098-3100.

Benson, S. W.; Cruickshank, F. R.; Golden, D. M.; Haugen, G. R.; O'Neil, H. E.; Rodgers, A. S.; Shaw, R.; Walsh, R. (1969). Additivity Rules for the Estimation of Thermochemical Properties. *Chem. Rev*., 69 (3), 279-324.

Berendsen, H. J. C.; Postma, J. P. M.; van Gunsteren, W. F. & Hermans, J. (1981). Interaction models for water in relation to protein hydration. In: *Intermolecular Forces*, B. Pulmann (Ed.), pp 331-342. D. Reidel Publishing Company, Dordrecht.

Bish, D. L. (1993). Rietveld refinement of the kaolinite structure at 1.5K. *Clays and Clay Miner.*, 41, 738-744.

Boehr, D.D.; Dyson, H. J.; Wright, P. E. (2006). An NMR Perspective on Enzyme Dynamics. *Chem. Rev.* 106, 3055–3079.

Boese, A. D.; Martin, J. M. L. (2004). Development of density functionals for thermochemical kinetics. *J. Chem. Phys*., 121, 3405-3416.

Boulet, P.; Greenwell, H. C.; Stackhouse, S. & Coveney, P.V. (2006). Recent advances in understanding the structure and reactivity of clays using electronic structure calculations. *J. Molecular Structure: THEOCHEM*, 762, 33–48.

Bredow, T.; Geudtner, G.; Jug, K. (2001). MSINDO parameterization for third-row transition metals. *J. Comput. Chem.*, 22, 861–887.

Brooks, B. R.; Bruccoleri, R. E.; Olafson, B. D.; States, D. J.; Swaminathan, S.; Karplus, M. (1983). CHARMM-a Program for Macromolecular Energy, Minimization, and Dynamics Calculations. *J. Comput. Chem.,* 4 (2), 187-217.

Bylaska, E. J.; Jong, W.A.d.; Kowalski, K.; Straatsma, T.P.; Valiev, M.; Wang, D.; Aprà, E.; Windus, T. L.; Hirata, S.; Hackler, M.T.; Zhao, Y.; Fan, P.-D.; Harrison, R.J.; Dupuis, M.; Smith, D. M. A.; Nieplocha, J.; Tipparaju, V.; Krishnan, M.; Auer, A. A.; Nooijen, M.; Brown, E.; Cisneros, G.; Fann, G. I.; Frücht, H.; Garza, J.; Hirao, K.; Kendall, R.; Nichols, J. A.; Tsemekhman, K.; Wolinsk, K.; Anchell, J.; Bernholdt, D.; Borowski, P.; Clark, T.; Clerc, D.; Dachsel, H.; Deegan, M.; Dyall, K.; Elwood, D.; Glendening, E.; Gutowski, M.; Hess, A.; Jaffe, J.; Johnson, B.; Ju, J.; Kobayashi, R.; Kutteh, R.; Lin, Z.; Littlefield, R.; Long, X.; Meng, B.; Nakajima, T.; Niu, S.; Pollack, L.; Rosing, M.; Sandrone, G.; Stave, M.; Taylor, H.; Thomas, G.; Lenthe, J.v.; Wong, A.; Zhang, Z. (2006*). NWChem, A Computational Chemistry Package for Parallel Computers,* Version 5.0. Pacific Northwest National Laboratory, Richland, Washington 99352-0999, USA (A modified version, 2006).

Bylaska, E. J.; de Jong, W. A.; Govind, N.; Kowalski, K.; Straatsma, T. P.; Valiev, M.; Wang, D.; Apra, E.; Windus, T. L.; Hammond, J.; Nichols, P.; Hirata, S.; Hackler, M. T.; Zhao, Y.; Fan, P.-D.; Harrison, R. J.; Dupuis, M.; Smith, D. M. A.; Nieplocha, J.;

Tipparaju, V.; Krishnan, M.; Wu, Q.; Van Voorhis, T.; Auer, A. A.; Nooijen, M.; Brown, E.; Cisneros, G.; Fann, G. I.; Fruchtl, H.; Garza, J.; Hirao, K.; Kendall, R.; Nichols, J. A.; Tsemekhman, K.; Wolinski, K.; Anchell, J.; Bernholdt, D.; Borowski, P.; Clark, T.; Clerc, C.; Dachsel, H.; Deegan, M.; Dyall, K.; Elwood, D.; Glendening, E.; Gutowski, M.; Hess, A.; Jaffe, J.; Johnson, B.; Ju, J.; Kobayashi, R.; Kutteh, R.; Lin, Z.; Littlefield, R.; Long, X.; Meng, B.; Nakajima, T.; Niu, S.; Pollack, L.; Rosing, M.; Sandrone, S.; Stave, M.; Taylor, H.; Thomas, G.; van Lenthe, J.; Wong, A.; Zhang, Z. *NWChem, A Computational Chemistry Package for Parallel Computers*, Version 5.1; Pacific Northwest National Laboratory: Richland, WA, 2007.

Cao, L. (2005). Immobilized Enzymes: science or art. *Current Opinion in Chemical Biology,* 9, 217–226.

Case, D. A.; Pearlman, D. A.; Caldwell, J. W.; T. E. Cheatham, I.; Ross, W. S.; Simmerling, C.; Darden, T.; Merz, K. M.; Stanton, R. V.; Cheng, A.; Vincent, J. J.; Crowley, M.; Ferguson, D. M.; Radmer, R.; Seibel, G. L.; Singh, U. S.; Weiner, P. K.; Kollman, P. A. (1997). *AMBER*, 5.0; University of California: San Francisco.

Casida, J. E.; Quistad, G. B. (1998). Golden age of insecticide research: past, present or future?. *Annu. Rev. Entomol*. 43, 1–16.

Cohen, N.; Benson, S. W. (1993). Estimation of heats of formation of organic compounds by additivity methods. *Chem. Rev.*, 93 (7), 2419-2438.

Coote, M. L.; Henry, D. J.(2005). Effect of substituents on radical stability in reversible addition fragmentation chain transfer polymerization: an ab initio study. *Macromolecules*, 38(4), 1415-1433.

Cornell, W. D.; Cieplak, P.; Bayly, C. I.; Gould, I. R.; Merz, K. M. Jr.; Ferguson, D. M.; Spellmeyer, D. C.; Fox, T.; Caldwell, J. W. & Kollman, P.A. (1995). A Second Generation Force Field for the Simulation of Proteins, Nucleic Acids and Organic Molecules, *J. Am. Chem. Soc.* 117, 5179-5197.

Coscarello, E. N.; Barbiric, D. A.; Castro, E. A.; Vico, R.V.; Bujan, E. I.; de Rossi, R. H. (2009). Comparative Analysis of Complexation of Pesticides (fenitrothion, methylparathion, parathion) and their Carboxylic Ester-Analogues by β-Cyclodextrin. Theoretical Semiempirical Calculations. *J. Structural Chemistry*, 50 (4), 705-713. ISSN: 0022-4766. Ed. Springer. J.Nº 10947.

Curtiss, L. A.; Raghavachari, K.; Redfern, P. C.; Pople, J. A. (1997). Assessment of Gaussian-2 and density functional theories for the computation of enthalpies of formation. *J. Chem. Phys.*, 106 (3), 1063-1079.

Curtiss, L. A.; Raghavachari, K.; Redfern, P. C.; Rassolov, V.; Pople, J. A. (1998). Gaussian-3 (G3) theory for molecules containing first and second-row atoms. *J. Chem. Phys.*, 109, 7764-7776.

Curtiss, L. A.; Raghavachari, K.; Redfern, P. C.; Pople, J. A. (2000a). Gaussian-3 theory using scaled energies. *J. Chem. Phys.*, 112 (3), 1125-1132.

Curtiss, L. A.; Raghavachari, K.; Redfern, P. C.; Pople, J. A. (2000b). Assessment of Gaussian-3 and density functional theories for a larger experimental test set. *J. Chem. Phys.*, 112, 7374-7383.

Curtiss, L. A.; Redfern, P. C.; Raghavachari, K.; Pople, J. A. (2001). Gaussian-3X (G3X) theory: Use of improved geometries, zero-point energies, and Hartree–Fock basis sets. *J. Chem. Phys.*, 114, 108-117.

David, R. L., Ed. (2007). CRC *Handbook of Chemistry and Physics*, 87th ed.; Taylor and Francis: Boca Raton, FL, ; http:/www.hbcpnetbase. com.

Dewar, M. J. S.; Zoebisch, E. G.; Healy, E. F. & Stewart, J. P. (1985) AM1: A new general purpose quantum mechanical molecular model, *J. Am. Chem. Soc.* 107, 3902-3909.

Dewar, M. J. S. & Merz, K. M.,Jr. (1988). AM1 parameters for zinc, *Organometallics* 7, 522-524.

Dewar, M. J. S., and Jie, C. (1989). AM1 parameters for phosphorus, *THEOCHEM* 187, 1-13.

Dorofeeva, O. V.; Moiseeva, N. F. (2006). Computational Study of the Thermochemistry of Organophosphorus(III) Compounds. *J. Phys. Chem. A* , 110, 8925-8932.

Duke, C. R.; Lubinsky, A. R.; Chang, S. C.; Lee, B. W.; Mark, P. (1977). Low-energy-electron-diffraction analysis of the atomic geometry of ZnO (10$\bar{1}$0). *Phys. Rev. B* , 15, 4865-4873.

Duke, C. B.; Meyer, R. J.; Paton, A.; Mark, P. (1978). Calculation of low-energy-electron-diffraction intensities from ZnO(10$\bar{1}$0). II. Influence of calculational procedure, model potential, and second-layer structural distortions. *Phys. Rev. B* , 18, 4225-4240.

Dyguda-Kazimierowicz E.; Sokalski, W.A. & Leszczynski, J. (2008). Gas-Phase Mechanisms of Degradation of Hazardous Organophosphorus Compounds: Do They Follow a Common Pattern of Alkaline Hydrolysis Reaction As in Phosphotriesterase? *J. Phys. Chem. B*, 112, 9982–9991.

Feigenbrugel, V.; Person, Calve, A. L.; Mellouki, S. L.; A.; Munoz, A.; Wirtz, K. (2006). Atmospheric fate of dichlorvos: Photolysis and OH-initiated oxidation studies. *Environ. Sci. Technol.*, 40 (3), 850-857.

Frisch, M. J.; Trucks, G. W.; Schlegel, H. B.; Gill, P. M. W.; Johnson, B. G.; Robb, M. A.; Cheeseman, J. R.; Keith, G. A.; Petersson, D. A.; Montgomery, J. A.; Al-Laham, M. A.; Zakrzewski, V. G.; Ortiz, J. V.; Foresman, J. B.; Cioslowski, J.; Stefanov, B. B.; Nanayakkara, A.; Challacombe, M.; Peng, C. Y.; Ayala, P. Y.; Chen, W.; Wong, M. W.; Andres, J. L.; Replogle, E. S.; Gomperts, R.; Martin, R. L.; Fox, D. J.; Binkley, J. S.; Defrees, G. J.; Baker, J.; Stewart, J. P.; Head-Gordon, M.; Gonzalez, C.; Pople, J. A. (1995); *Gaussian 94 (Revision A.1); Gaussian, Inc.: Pittsburgh, PA*.

Frisch, M. J.; Trucks, G. W.; Schlegel, H. B.; Scuseria G. E.; Robb, M. A.; Cheeseman, J. R.; Zakrzewski, V. G. Jr.; Montgomery, J. A.; Stratmann, R. E.; Burant J. C.; Dapprich, S.; Millam, J. M.; Daniels, A. D.; Kudin, K. N.; Strain, M. C.; Farkas, O.; Tomasi, J.; Barone, V.; Cossi, M.; Cammi, R.; Mennucci, B.; Pomelli, C.; Adamo, C.; Clifford, S.; Ochterski, J.; Petersson, G. A.; Ayala, P.Y.; Cui, Q.; Morokuma, K.; Malick, D. K.; Rabuck, A. D.; Raghavachari, K.; Foresman, J. B.; Cioslowski, J.; Ortiz, J. V.; Stefanov, B. B.; Liu, G.; Liashenko, A.; Piskorz, P.; Komaromi, I.; Gomperts, R.; Martin, R. L.; Fox, D. J.; Keith, T.; Al-Laham, M. A.; Peng, C. Y.; Nanayakkara, A. ; Gonzalez, C.; Challacombe, M.; Gill, P. M. W.; Johnson, B.; Chen, W.; Wong, M. W.; Andres, J. L.; Gonzalez, C.; Head-Gordon, M.; Replogle, E. S.; Pople, J. A. (1998); *Gaussian 98 (Revision A.6); Gaussian, Inc.: Pittsburgh, PA*.

Frisch, M. J.; Trucks, G. W.; Schlegel, H. B.; Scuseria, G. E.; Robb, M. A.; Cheeseman, J. R.; Montgomery J. A., Jr.; Vreven, T.; Kudin, K. N.; Burant, J. C.; Millam, J. M.; Iyengar, S. S.; Tomasi, J.; Barone, V.; Mennucci, B.; Cossi, M.; Scalmani, G.; Rega, N.; Petersson, G. A.; Nakatsuji, H.; Hada, M.; Ehara, M.; Toyota, K.; Fukuda, R.;

Hasegawa, J.; Ishida, M.; Nakajima, T.; Honda, Y.; Kitao, O.; Nakai, H.; Klene, M.; Li, X.; Knox, J. E.; Hratchian, H. P.; Cross, J. B.; Bakken, V.; Adamo, C.; Jaramillo, J.; Gomperts, R.; Stratmann, R. E.; Yazyev, O.; Austin, A. J.; Cammi, R.; Pomelli, C.; Ochterski, J. W.; Ayala, P. Y.; Morokuma, K.; Voth, G. A.; Salvador, P.; Dannenberg, J. J.; Zakrzewski, V. G.; Dapprich, S.; Daniels, A. D.; Strain, M. C.; Farkas, O.; Malick, D. K.; Rabuck, A. D.; Raghavachari, K.; Foresman, J. B.; Ortiz, J. V.; Cui, Q.; Baboul, A. G.; Clifford, S.; Cioslowski, J.; Stefanov, B. B.; Liu, G.; Liashenko, A.; Piskorz, P.; Komaromi, I.; Martin, R. L.; Fox, D. J.; Keith, T.; Al.Laham, M. A.; Peng, C. Y.; Nanayakkara, A.; Challacombe, M.; Gill, P. M. W.; Johnson, B.; Chen, W.; Wong, M. W.; Gonzalez, C.; Pople, J. A. (2004). *Gaussian 03, Revision X.0X. Gaussian, Inc., Wallingford CT, 2004.*

Fuxreiter, M.; Warshel, A. (1998). Origin of the Catalytic Power of Acetylcholinesterase: Computer Simulation Studies. *J. Am. Chem. Soc.*, 120, 183-194.

Fukui, K. (1981). The path of chemical reactions: The IRC approach. *Acc. Chem. Res.*, 14 (12), 363-368.

Gomes, D. E. B.; Lins, R. D.; Pascutti, P. G.; Straatsma, T. P.; Soares, T. A. (2008). Molecular Models to Emulate Confinement Effects on the Internal Dynamics of Organophosphorous Hydrolase. *Lecture Notes in Bioinformatics*, 5167, 68-78. A.L.C. Bazzan, M. Craven, and N.F. Martins (Eds.). Springer-Verlag Berlin Heidelberg.

Gorb, L.; Lutchyn, R.; Zub, Yu.; Leszczynska, D.; Leszczynski, J. (2006). The origin of the interaction of 1,3,5-trinitrobenzene with siloxane surface of clay minerals. *J. Molecular Structure: THEOCHEM*, 766, 151–157.

Grimme, S. (2003). Improved second-order Møller–Plesset perturbation theory by separate scaling of parallel- and antiparallel-spin pair correlation energies. *J. Chem. Phys.*, 118, 9095-9102.

Grimme, S. (2006). Semiempirical hybrid density functional with perturbative second-order correlation. *J. Chem. Phys.*, 124, 034108-034123.

Haderlein, S. B.; Schwarzenbach, R. P. (1993). Adsorption of substituted nitrobenzenes and nitrophenols to mineral surfaces. *Environ. Sci. Technol.*, 27(2), 316-26.

Haderlein, S. B.; Weissmahr, K. W.; Schwarzenbach, R. P. (1996). Specific adsorption of nitroaromatic explosives and pesticides to clay minerals. *Environ. Sci. Technol.*, 30 (2), 612-622.

Harrison, M. A. J.; Barra, S.; Borghesi, D.; Vione, D.; Arsene, C.; Olariu, R. L. (2005). Nitrated phenols in the atmosphere: a review. *Atmos. Environ.*, 39, 231-248.

Hehre, W. J.; Radom, L.; Schleyer, P. v. R. & Pople, J. A. (1986). *Ab initio molecular orbital theory*, Wiley, New York.

Hemelsoet, K.; Van Durme, F.; Van Speybroeck, V.; Reyniers, M-F & Waroquier, M. (2010). Bond Dissociation Energies of Organophosphorus Compounds: an Assessment of Contemporary Ab Initio Procedures. *J. Phys. Chem. A*, *114,* 2864–2873

Hodgson, J. L.; Coote, M. L. (2005). Effects of Substituents on the Stability of Phosphoranyl Radicals. *J. Phys. Chem. A*, 109, 10013- 10021.

Hofer, W. (1981). Chemistry of metrifonate and dichlorvos. *Acta Pharmacol. Toxicol.*, 49 (Suppl. 5), 7-14.

HyperChem 7 for Windows, Hypercube Inc., 2002.

Janssen, R. H. C.; Theodorou, D. N.; Raptis, S.; Papadopoulos, M. G. (1999). Molecular simulation of static hyper-Rayleigh scattering: A calculation of the depolarization ratio and the local fields for liquid nitrobenzene. *J. Chem. Phys*., 111, 9711-9719.

Jensen, F. (1999*): Introduction into computational chemistry*. John Wiley, ISBN 0471984256, England.

Jorge, M.; Gulaboski, R.; Pereira, C. M.; Cordeiro, M. (2006). Molecular dynamics study of nitrobenzene and 2-nitrophenyloctyl ether saturated with water. *Mol. Phys.*, 104, 3627-3634.

Jorgensen, W. L.; Tirado-Rives, J. (1988). The OPLS Force Field for Proteins. Energy Minimizations for Crystals of Cyclic Peptides and Crambin. *J. Am. Chem. Soc.,* 110, 1657–1666.

Jorgensen, W.L.; Maxwell. D.S.; Tirado-Rives, J. (1996). Development and Testing of the OPLS All-Atom Force Field on Conformational Energetics and Properties of Organic Liquids. *J. Am. Chem. Soc.,* 118 (45), 11225–11236.

Jung, Y.; Lochan, R. C.; Dutoi, A. D.; Head-Gordon, M. (2004). Scaled opposite-spin second order Møller–Plesset correlation energy: An economical electronic structure method. *J. Chem. Phys*., 121 (20), 9793-9803.

Kamiya, M.; Nakamura, K.; Sasaki, C.(1995). Inclusion effects of β-cyclodextrins on the hydrolysis of organophosphorus pesticides. *Chemosphere,* 30 (4), 653-660.

Klauda, J. B.; Pastor, R. W.; Brooks, B. R. (2005a). Adjacent gauche stabilization in linear alkanes: Implications for polymer models and conformational analysis. *J. Phys. Chem. B*, 109 (33), 15684–15686.

Klauda, J. B.; Brooks, B. R.; MacKerell, A. D. Jr.; Venable, R. M.; Pastor, R. W. (2005b). An Ab Initio Study on the Torsional Surface of Alkanes and its Effect on Molecular Simulations of Alkanes and a DPPC Bilayer. *J. Phys. Chem. B* , 109, 5300-5311.

Klauda, J. B. & Brooks, B. R. (2008). CHARMM Force Field Parameters for Nitroalkanes and Nitroarenes. *J. Chem. Theory Comput*., 4, 107-115.

Koča, J.; Zhan, C.-G.; Rittenhouse, R.C. & Ornstein, R.L. (2001). Mobility of the Active Site Bound Paraoxon and Sarin in Zinc-Phosphotriesterase by Molecular Dynamics Simulation and Quantum Chemical Calculation. *J. Am. Chem. Soc*., 123, 817-826.

Kwasnieski, O.; Verdier, L.; Malacria, M. & Derat, E. (2009). Fixation of the Two Tabun Isomers in Acetylcholinesterase: A QM/MM Study. *J. Phys. Chem. B*, 113, 10001–10007.

Leach, A. R. (2001). *Molecular Modelling, principles and applications*, 2nd Ed. 2001, Pearson Education Limited, ISBN 0-582-38210-6, England.

Lee, C.; Yang, W.; Parr, R. G. (1988). Development of the Colle-Salvetti correlation-energy formula into a functional of the electron density. *Phys. Rev. B*, 37, 785-789.

Lei, C.; Shin, Y.; Liu, J.; Ackerman, E. J. (2002). Entrapping enzyme in a functionalized nanoporous support. *J. Am. Chem. Soc.,* 124, 11242–11243.

Lei, C.; Shin, Y.; Liu, J.; Ackerman, E. J. (2007). Synergetic effects of nanoporous support and urea on enzyme activity. *Nano Letters,* 7, 1050–1053.

Lindahl, E.; Hess, B.; Spoel, D.v.d. (2001). GROMACS 3.0: A package for molecular simulation and trajectory analysis. *J. Molecular Modeling*, 7, 306–317.

MacKerell, A. D., Jr. (2001). Atomistic Models and Force Fields. In: *Computational Biochemistry and Biophysics*; Becker, O. M., MacKerell, A. D., Jr., Roux, B., Watanabe, M., Eds., p 7-38, Marcel Dekker: New York.

MacKerell, A. D. Jr., (2004). Empirical force fields for biological macromolecules: Overview and issues. *J. Comput. Chem.*, 25, 1584-1604.

MacKerell, A. D. Jr. (2005). Interatomic Potentials: Molecules. In: *Handbooks of Material* Modeling; Yip, S., Ed. p 509-525; Springer: The Netherlands.

Manunza, B.; Deiana, S.; Pintore, M..; Delogu, G.; Gessa, C. (1998). A Molecular Dynamics Investigation on the Inclusion of Chiral Agrochemical Molecules in β-Cyclodextrin. Complexes with Dichlorprop, 2-Phenoxypropionic Acid and Dioxabenzofos. *Pestic. Sci.*, 54, 68-74.

Mennucci, B.;Tomasi, J.; Cammi, R.; Cheeseman, J.R.; Frisch, M.J.; Devlin, F.J.; Gabriel, S.; Stephens, P.J. (2002). Polarizable Continuum Model (PCM) Calculations of Solvent Effects on Optical Rotations of Chiral Molecules, *J. Phys. Chem. A.*, 106, 6102-6113.

Michael, D.; Benjamin, I. (1998). Molecular dynamics simulation of the water-nitrobenzene interface. *J. Electroanal. Chem.*, 450 (2), 335-345.

Michalkova, A.; Paukku, Y.; Majumdar, D.; Leszczynski, J. (2007). Theoretical study of adsorption of tabun on calcium oxide clusters. *Chem. Phys. Lett.*, 438, 72-77.

Murphy, K. C.; Cooper, R. J.; Clark, J. M. (1996). Volatile and dislodgeable residues following trichlorfon and isazofos application to turfgrass and implications for human exposure. *Crop Sci.*, 36 (6), 1446-1454.

Nair, R. K.; Kadam, M. M.; Sawant, M. R.(2006). Effect on the Solubility, Wettability, and Dispersibility of the β-CD-Deltamethrin Inclusion Complex in Presence of Mixed Surfactant (C_{14}MEA/AOS) Blend. *J. Disper. Sci. Tech.* 27 (7) , 1015 – 1019. Taylor & Francis Eds. ISSN: 1532-2351.

Omburo, G. A.; Kuo, J. M.; Mullins, L. S.; Raushel, F. M. (1992). Characterization of the zinc binding site of bacterial phosphotriesterase. *J. Biological Chemistry,* 267, 13278–13283.

Osa, T.; Suzuki, I. (1996). In: *Comprehensive Supramolecular Chemistry (Vol. 3) Cyclodextrins*. Eds. J. Szejtli and T. Osa., pp 367 – 400. Pergamon, Oxford.

Paukku, Y.; Michalkova, A. & Leszczynski, J. (2008). Adsorption of dimethyl methylphosphonate and trimethyl phosphate on calcium oxide: an ab initio study. *J. Struct. Chem.*, 19 (2), 307-320.

Paukku, Y.; Michalkova, A. & Leszczynski, J. (2009). Quantum-Chemical Comprehensive Study of the Organophosphorus Compounds Adsorption on Zinc Oxide Surfaces. *J. Phys. Chem. C* 2009, 113, 1474–1485

Pelmenschikov, A. & Leszczynski, J. (1999). Adsorption of 1,3,5-Trinitrobenzene on the Siloxane Sites of Clay Minerals: Ab Initio Calculations of Molecular Models. *J. Phys. Chem. B,* 103, 6886-6890.

Pettigrew, L. C.; Bieber, F.; Lettiere, J.; Wermeling, D. P.; Schmitt, F. A.; Tikhtrman, A. J.; Ashford, J. W.; Smith, C. D.; Wekstein, D. R.; Markesbery, W. R.; Orazem, J.; Ruzicka, B. B.; Mas, J.; Gulanski, B. (1998). Pharmacokinetics, pharmacodynamics, and safety of metrifonate in patients with Alzheimer's disease. *J. Clin. Pharmacol.*, 38 (3), 236-245.

Pilcher, G. (1990). Thermochemistry of phosphorus(III) compounds. In: *The Chemistry of Organophosphorus Compounds*; Hartley, F. R., Ed.; Vol. 1, p 127-136. J. Wiley & Sons, New York.

Price, M. L. P.; Ostrovsky, D.; Jorgensen, W. L. (2001). Gas-phase and liquid-state properties of esters, nitriles, and nitro compounds with the OPLS-AA force field. *J. Comput. Chem*., 22, 1340-1352.

Price, D. J.; Brooks, C. L. (2005). Detailed considerations for a balanced and broadly applicable force field: A study of substituted benzenes modeled with OPLS-AA. *J. Comput. Chem*., 26 (14), 1529-1541.

Raushel, F. M. (2002). Bacterial detoxification of organophosphate nerve agents. *Curr. Opin. Microbiol*., 5, 288–295.

Richards, R.; Li, W.; Decker, S.; Davidson, C.; Koper, O.; Zaikovski, V.; Volodin, A.; Rieker, T.; Klabunde, K. J. (2000). Consolidation of Metal Oxide Nanocrystals. Reactive Pellets with Controllable Pore Structure That Represent a New Family of Porous, Inorganic Materials. *J. Am. Chem. Soc*., 122 (20), 4921-4925.

Rochu, D.; Renault, F.; Viguille, N.; Crouzier, D.; Froment, M. T.; Masson, P. (2004). Contribution of the active-site metal cation to the catalytic activity and to the conformational stability of phosphotriesterase: temperature- and pH-dependence. *Biochemical Journal,* 380, 627–633.

Schaftenaar, G.; Noordik, J. H. (2000). MOLDEN: a pre- and post-processing program for molecular and electronic structures. *J. Comput.-Aided Mol. Des*. 14, 123-134.

Schmidt, M.W.; Baldridge, K. K.; Boatz, J. A.; Elbert, S. T.; Gordon, M. S.; Jensen, J. J.; Koseki, S.; Matsunaga, N.; Nguyen, K. A.; Su, S.; Windus, T. L.; Dupuis, M.; Montgomery, J. A. (1993). GAMESS Version 21 Nov. 1995, *J. Comput. Chem*. 14 , 1347-1363.

Scholz, F.; Schroder, U.; Gulaboski, R. (2005). *Electrochemistry of Immobilized Particles and Droplets*; Springer: Berlin, Heidelberg, New York. ISBN 3-540-22005-4.

Schwabe, T.; Grimme, S. (2006). Towards chemical accuracy for the thermodynamics of large molecules: new hybrid density functionals including non-local correlation effects. *Phys. Chem. Chem. Phys*., 8 (38), 4398-4401.

Silman, I. & Sussman, J. L. (2005). Acetylcholinesterase: "Classical" and "non-classical" functions and pharmacology. *Curr Opin. Pharmacol.,* 5, 293-302.

Smith, W. & Forester, T. R. (1994). *DLPOLY2, package of molecular simulation routines*, copyright the Council for the Central Laboratory of the Research Councils, Daresbury Laboratory, Warrington U.K. (1994-6).

Soares, T. A.; Osman, M.; Straatsma, T. P. (2007). Molecular dynamics of organophosphorous hydrolases bound to the nerve agent soman. *J. Chemical Theory and Computation,* 3, 1569–1579.

Sokalski, W.A.; Roszak, S.; Pecul, K. (1988). An efficient procedure for decomposition of the SCF interaction energy into components with reduced basis set dependence. *Chem. Phys. Lett*., 153, 153-159.

Spain, J. C. (1995). Biodegradation of Nitroaromatic Compounds. *Annu. Rev. Microbiol*., 49, 523-555.

Staroverov, V. N.; Scuseria, G. E.; Tao, J.- M.; Perdew, J. P. (2003). Comparative assessment of a new nonempirical density functional: Molecules and hydrogen-bonded complexes. *J. Chem. Phys.*, 119 (23), 12129-12137.

Stewart, J. J. P. (1989 a). Optimization of Parameters for Semi-Empirical Methods. I-Method. *J. Comput. Chem.*, 10, 209-220.

Stewart, J. J. P. (1989b). Optimization of Parameters for Semiempirical Methods. II. Applications. *J. Comput. Chem.*, 10, 221-264.

Svensson, M.; Humbel, S.; Froese, R.D.J.; Matsubara, T.; Sieber, S. & Morokuma, K. (1996). ONIOM. A Multilayered Integrated MO + MM Method for Geometry Optimisations and Smgle Point Energy Predictions. A Test for Diels-Alder Reactions and $Pt(P(t\text{-}Bu)_3)_2+H_2$ Oxidative Addition. *J. Phys. Chem.*,100, 19357-19363.

Szejtli, J.(2004). Past, present, and future of cyclodextrin research. *Pure Appl. Chem.* 76 (10), 1825–1845.

Tao, J. -M.; Perdew, J. P.; Staroverov, V. N.; Scuseria, G. E. (2003). Climbing the Density Functional Ladder: Nonempirical Meta- Generalized Gradient Approximation Designed for Molecules and Solids. *Phys. Rev. Lett.*, 91(14), 146401/1-4.

Vico R.V., Buján E.I., de Rossi R.H. (2002). Effect of cyclodextrin on the hydrolysis of the pesticide fenitrothion [*O,O*-dimethyl *O*-(3-methyl-4-nitrophenyl)phosphorothioate]. *J. Phys. Org. Chem.*15 (12), 858– 862.

Wahab, H.S.; Koutselos A. D. (2009). Computational modeling of the adsorption and •OH initiated photochemical and photocatalytic primary oxidation of nitrobenzene. *J. Mol. Model*., 15, 1237–1244.

Warshel, A.; Naray-Szabo, G.; Sussman, F.; Hwang, J. K. (1989). How do serine proteases really work?. *Biochemistry*, 28, 3629-3637.

Weiner, S. J.; Kollman, P. A.; Case, D.A.; Singh, U. C.; Ghio, C.; Alagona, G.; Profeta, S. & Weiner, P. (1984). A New Force Field for Molecular Mechanical Simulation of Nucleic Acids and Proteins. *J. Am. Chem. Soc*., 106, 765-784.

Weissmahr, K. W.; Haderlein, S. B.; Schwarzenbach, R. P. (1997). In situ spectroscopic investigations of adsorption mechanisms of nitroaromatic compounds at clay minerals. *Environ. Sci. Technol.*,31(1), 240-247.

Werner, H.-J.; Knowles, P. J.; Amos, R. D.; Bernhardsson, A.; Berning, A.; Celani, P.; Cooper, D. L.; Deegan, M. J. O.; Dobbyn, A. J.; Ecker, F.; Hampel, C.; Hetzer, G.; Knowles, P. J.; Korona, T.; Lindh, R.; Lloyd, A. W.; McNicholas, S. J.; Manby, F. R.; Meyer. W.; Mura, M. E.;Nicklass, A.; Palmieri, P.; Pitzer, R.; Rauhut, G.; Schutz, M.; Schumann, U.; Stoll, H.; Stone, A. J.; Tarroni, R.; Thorsteinsson, T. (2002). *MOLPRO 2002.6*; University of Birmingham: Birmingham, U.K..

Wong, K-.Y. & Gao, J. (2007). The Reaction Mechanism of Paraoxon Hydrolysis by Phosphotriesterase from Combined QM/MM Simulations. *Biochemistry*, 46, 13352-13369

Woods, R. J.; Dwek, R. A.; Edge, C. J. & Fraser-Reid, B. (1995). Molecular mechanical and molecular dynamical simulations of glycoproteins and oligosaccharides. 1. GLYCAM- 93 parameter development, *J. Phys. Chem*., 99, 3832-3846.

Yun, K.-H.; Yun, K.-Y.; Cha, G.-Y.; Lee, B.-H.; Kim, J.-C.; Lee, D.-D.; Huh, J.-S. (2005). Gas Sensing Characteristics of ZnO-doped SnO_2 Sensors for Simulants of the Chemical

Agents. *Mater. Sci. Forum* , Vols. *486-487*, pp.9-12 in Eco-Materials Processing & Design VI. DOI: 10.4028/www.scientific.net/MSF.486-487.9

Zhang, Q.; Qu, X. ; Wang, W.(2007). Mechanism of OH-Initiated Atmospheric Photooxidation of Dichlorvos: A Quantum Mechanical Study. *Environ. Sci. Technol.*, 41, 6109-6116.

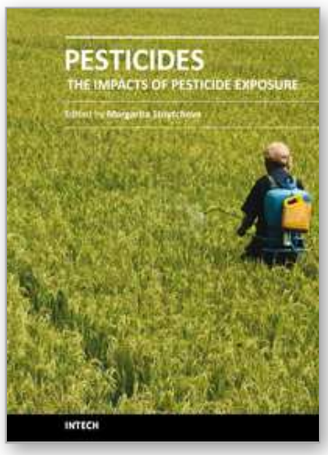

Pesticides - The Impacts of Pesticides Exposure
Edited by Prof. Margarita Stoytcheva

ISBN 978-953-307-531-0
Hard cover, 446 pages
Publisher InTech
Published online 21, January, 2011
Published in print edition January, 2011

Pesticides are supposed to complete their intended function without â€œany unreasonable risk to man or the environmentâ€. Pesticides approval and registration are performed â€œtaking into account the economic, social and environmental costs and benefits of the use of any pesticideâ€. The present book documents the various adverse impacts of pesticides usage: pollution, dietary intake and health effects such as birth defects, neurological disorders, cancer and hormone disruption. Risk assessment methods and the involvement of molecular modeling to the knowledge of pesticides are highlighted, too. The volume summarizes the expertise of leading specialists from all over the world.

How to reference
In order to correctly reference this scholarly work, feel free to copy and paste the following:

Ethel N. Coscarello, Ruth Hojvat, Dora A. Barbiric and Eduardo A. Castro (2011). The Contribution of Molecular Modeling to the Knowledge of Pesticides, Pesticides - The Impacts of Pesticides Exposure, Prof. Margarita Stoytcheva (Ed.), ISBN: 978-953-307-531-0, InTech, Available from: http://www.intechopen.com/books/pesticides-the-impacts-of-pesticides-exposure/the-contribution-of-molecular-modeling-to-the-knowledge-of-pesticides

INTECH
open science | open minds

InTech Europe
University Campus STeP Ri
Slavka Krautzeka 83/A
51000 Rijeka, Croatia
Phone: +385 (51) 770 447
Fax: +385 (51) 686 166
www.intechopen.com

InTech China
Unit 405, Office Block, Hotel Equatorial Shanghai
No.65, Yan An Road (West), Shanghai, 200040, China
中国上海市延安西路65号上海国际贵都大饭店办公楼405单元
Phone: +86-21-62489820
Fax: +86-21-62489821

IntechOpen